

Glacio-Kinematic Analysis of ERS-1/2 SAR Data of the Antarctic Ice Shelf Ekströmisen and the Adjoining Inland Ice Sheet

By Uwe Müller¹, Henner Sandhäger², Jörn Sievers¹ and Norbert Blindow²

Summary: ERS-1/2 SAR intensity and phase difference imagery of the Antarctic ice shelf Ekströmisen and the adjoining inland ice sheet are analysed from the aspect of glacio-kinematics. The investigation is mainly focused on a classification of the back-scattered radar signal and of the derived interferometric fringe patterns and their assignment to features of the ice body and its flow dynamics. The latter item is performed by including auxiliary data from terrestrial in-situ measurements, airborne soundings and altimetry, and optical satellite imagery. The interpretation provides new findings on the distribution of surface-crevasse patterns, the properties of the surface layer, the flow regime, and the stress conditions within the ice body. The course of the grounding line of Ekströmisen is remapped. The possibility of a correlation between surface undulations in the catchment area and sliding processes at the ice/bedrock transition is discussed. Investigations on the dynamics of the ice front result in an estimate of its advance and of a classification of the different coastal sectors as to the extent and periodicity of calving events. All in all, it becomes evident that the analysis of ERS-1/2 SAR image data constitutes an efficient procedure for detailed examinations of ice-covered areas and is therefore also suitable for monitoring those Antarctic regions rated as particularly sensitive to climate induced changes.

Zusammenfassung: ERS-1/2-SAR-Intensitäts- und -Phasendifferenzbilder des antarktischen Schelfeises Ekströmisen und der angrenzenden Inlandeisbereiche werden unter glaziokinematischen Gesichtspunkten interpretiert. Schwerpunkte sind eine Klassifikation der rückgestreuten und reflektierten Radarsignale bzw. der abgeleiteten interferometrischen Fringe-Muster und deren Zuordnung zu Merkmalen des Eiskörpers und seiner Fließdynamik. Letzteres erfolgt unter Einbeziehung von terrestrischen in-situ-Messungen, flugzeuggetragenen Eisdicken- und Altimetermessungen und optischen Satellitenbildern. Die Interpretation liefert neue Erkenntnisse über die Verteilung oberflächennaher Bruchstrukturen im Schelfeis, die Eigenschaften der Deckschicht, das Fließregime und die Spannungsverhältnisse im Eiskörper. Der Verlauf der Aufsetzlinie des Ekströmisen wird neu kartiert. Ein möglicher Zusammenhang zwischen Oberflächenundulationen in den Einzugsgebieten und Gleitprozessen an der Grenzfläche Eis/Fels wird diskutiert. Aus Untersuchungen zur Dynamik der Eisfront resultieren eine Abschätzung kantennaher Fließgeschwindigkeiten und eine Einteilung der Küstenabschnitte nach Ausmaß und Periodizität der Kalbungsvorgänge. Insgesamt zeigt sich, daß die Analyse von ERS-1/2-SAR-Bilddaten eine effiziente Methode zur detaillierten flächenhaften Untersuchung eisbedeckter Gebiete ist und sich deshalb u.a. auch für ein Monitoring solcher Bereiche der Antarktis eignet, die als besonders sensitiv gegenüber klimabedingten Veränderungen eingestuft werden.

INTRODUCTION

Floating ice shelves border about 44 % of the Antarctic coast line and comprise approx. 11 % of the area of the entire ice sheet (DREWRY 1983). A large part of the ice masses emanating from

the inland ice-sheet regions is supplied to the ice shelves whose stability mainly results from their lateral coupling to the inland ice in bays and to ice rises or ice rumples resting on shoals within or at the seaward edges of the floating portions of the ice body.

Ice shelves constitute in two senses active components in the global climate system. It is on the one hand assumed that by exerting back-pressure the ice shelves are a contributory determinant to the dynamics of the adjacent inland ice sheet and are therefore partly responsible for its stabilization (e.g. MACAYEAL 1987); secondly, mass exchange with the ocean takes place at the ice-shelf base by melting and accumulation of marine ice, respectively. These processes influence the mass balance and the dynamics of the ice body as well as the ocean circulation in the sub-ice shelf cavities. Thus, the ice/ocean interactions also contribute to the formation and modification of water masses such as Antarctic Bottom Water which advances as far as the northern hemisphere and plays an important role with regard to the ventilation of the oceans (EMERY & MEINCKE 1986).

In order to get a better understanding of ice-shelf dynamics and of the question how sensitive ice shelves are responding to climate changes, satellite data have been used over approx. the last 20 years. This method was for instance incorporated by DOAKE & VAUGHAN (1991) and ROTT et al. (1996) in investigations on the progressive disintegration of different ice shelves of the Antarctic Peninsula as a consequence of the proven regional atmospheric warming there (VAUGHAN & DOAKE 1996).

In this study, we refer to a combined analysis of ERS-1/2 SAR intensity and differential phase images for the purpose of a detailed examination of the Antarctic ice shelf Ekströmisen and the adjacent ice-sheet regions.

The area of investigation Ekströmisen

Ekströmisen (Fig. 1) covers an area of about 8700 km² (extracted from IfAG 1989) and is one of the comparatively small ice shelves in the Atlantic coastal zone of East Antarctica. To the south Ekströmisen is bounded by the grounded ice masses of Ritscherflya, which is a marginal region of the East Antarctic Ice Sheet. The western and eastern boundaries of the ice shelf are formed by the dome-shaped ice caps Auståsen, Søråsen, and Halvfarryggen, respectively. Each of them is characterized by

¹ Bundesamt für Kartographie und Geodäsie, Richard-Strauss-Allee 11, D-60598 Frankfurt a. Main, Germany

² Institut für Geophysik, Westfälische Wilhelms-Universität Münster, Corrensstraße 24, D-48149 Münster, Germany

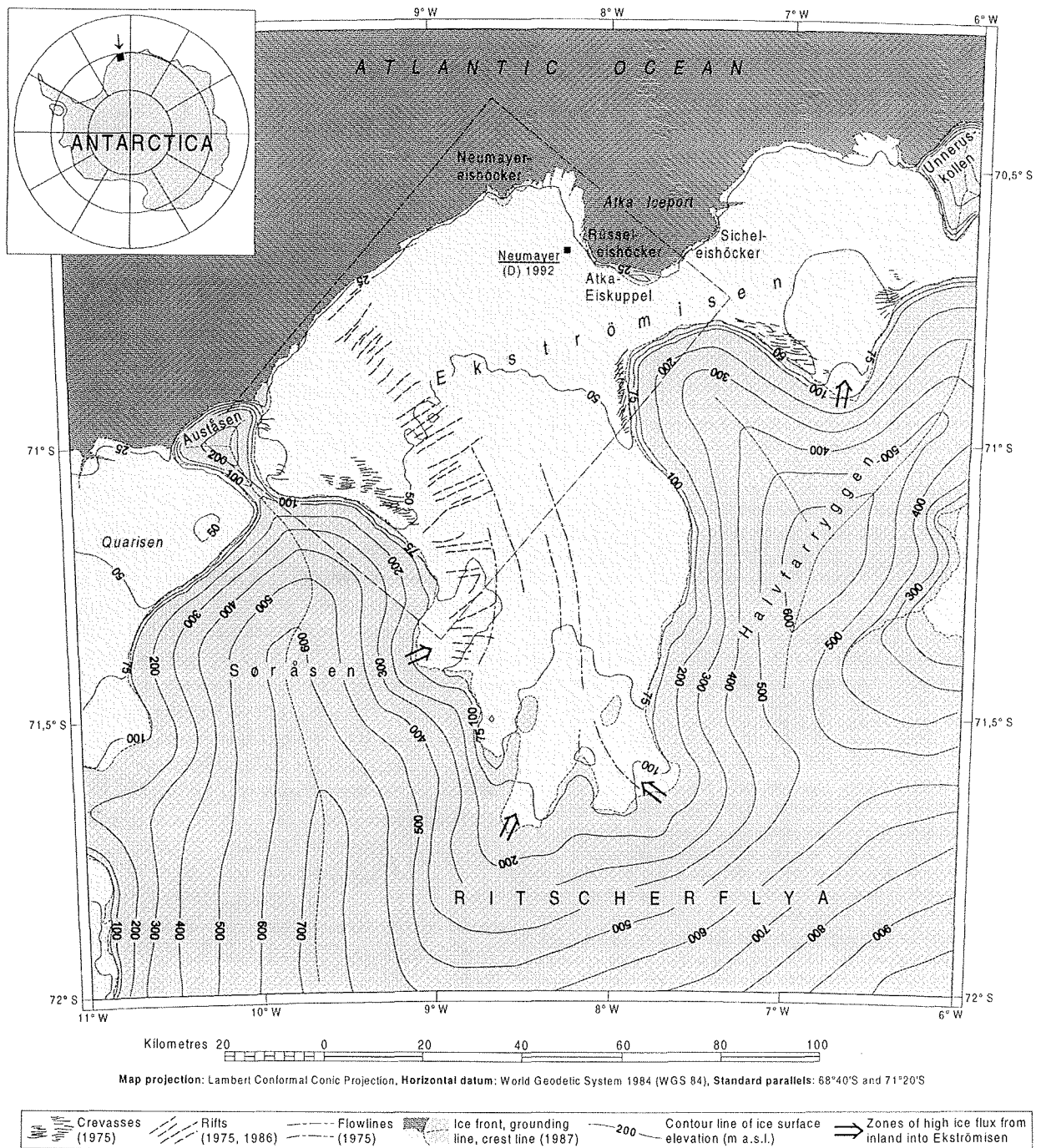


Fig. 1: General topographic map of Ekströmsen and the adjacent ice-sheet and ice-shelf regions. Indicated surface features, such as crevasses, rifts, flowlines, grounding lines, crest lines, and the ice front result from classifications on Landsat MSS imagery (IfAG 1989, IfAG 1993, IfAG/AWI 1994). Surface elevations have been derived from airborne altimetry (SANDHÄGER & BLINDOW 2000). Arrows indicate zones of high ice flux from inland into Ekströmsen. The broken rectangle marks the position of the ERS-1 SAR intensity image shown in Figure 2.

Abb. 1: Topographische Übersichtskarte des Ekströmsen und der angrenzenden Inlandeis- und Schelfeisbereiche. Die eingetragenen Oberflächenmerkmale wie Spalten, Schelfeisgräben, Fließlinien, Aufsetzlinien, Kammlinien und die Eisfront resultieren aus Interpretationen von Landsat-MSS-Aufnahmen (IfAG 1989, IfAG 1993, IfAG/AWI 1994). Die Oberflächenhöhen sind aus Flugaltimetriedaten abgeleitet (SANDHÄGER & BLINDOW 2000). Markiert sind die vier Hauptzuflussbereiche von Inlandeismassen in das Ekströmsen (Pfeile) sowie die Lage des in Abbildung 2 dargestellten ERS-1-SAR-Intensitätsbildes (gestricheltes Rechteck).

an individual flow regime largely independent of the movement in the adjacent ice-sheet region. The northwestern part of Halvfarryggen and Atka-Eiskuppel - an ice rise bordering on the Atka Iceport in the south - subdivide Ekströmsen into a small eastern part (~2000 km²) and a major western part (~6700 km²). The two

German scientific stations Georg-von-Neumayer and Neumayer, which were opened there in 1981 and 1991, respectively, have been used as bases for several expeditions to the ice shelf and the hinterland.

The main catchment area of the eastern part of Ekströmsisen is the (~1400 km² large northern slope of the Halvfarryggen ice dome, whereas the western part of the ice shelf is mainly fed by ice masses emanating from a (~15,000 km² large region of Ritscherflya over the southernmost section of the grounding line (DREWRY 1983, MAYER 1996, SANDHÄGER & BLINDOW 2000). The horizontal flow direction of southwestern Ekströmsisen is therefore orientated approximately from south to north before it turns gradually towards northwest with decreasing distance from the ice front. The flow regime is additionally influenced by the topography of the laterally adjacent ice caps as well as by the mass discharge from these ice caps into the ice shelf. As a result of that, several marginal zones of Ekströmsisen are characterized by high longitudinal and/or shear stresses in the ice which cause the formation of fractures, such as crevasses or shear zones (IfAG 1989). Figure 1 shows the distribution of crevasses and other surface features, such as flowlines, the ice front, grounding lines, and crest lines. The represented pattern of surface features results from an interpretation of optical satellite images recorded in 1975, 1986, and 1987 with the optical sensor MSS (Multispectral Scanner) of the satellites Landsat-2 and -5 (IfAG 1989, IfAG 1993, IfAG/AWI 1994).

On the basis of data that were recorded in 1996 with the actively imaging radar system of ERS-1 and -2 (Tab. 1) an obviously more detailed and more comprehensive classification and mapping of ice-surface features is achieved. Since those systems additionally supply data on the prevailing glacial conditions beneath the ice surface, the distribution of near surface structures and surface undulations, the constitution of the snowpack, the position of the grounding line as well as different characteristics of the flow regime are also investigated. Furthermore, the changes in position and shape of the ice front of Ekströmsisen between 1987 and 1996 are analysed.

ERS-1/2 SAR data

Whereas optical satellite imagery renders exclusively topographic features and surface structures, the radar signal emitted by ERS-1/2 can penetrate as far as some tens of metres into the ice body before being back-scattered or reflected. The depth of penetration depends above all on the content of liquid water as well as on the density and composition of the near surface layers (SAURER et al. 1998). In vast areas of the Antarctic

ice sheet a cold snowpack does exist which is unmodified by meltwater. The thickness of this surface layer composed of dry snow is determined by the rate of precipitation and the surface temperature. With increasing depth and load the snow transforms into firn (settled snow older than 1 year) as a consequence of the diagenesis and metamorphism, and later into consolidated ice (PATERSON 1994). If in warmer coastal regions a seasonal change of surface melting and subsequent refreezing occurs, ice layers and lenses may form in the snowpack.

Since homogeneous fine-grained dry snow shows only little scattering for radar radiation, a thin snow layer of some metres is nearly transparent for the radar signal (SAURER et al. 1998). The recorded signal then results primarily from the scattering and reflection properties of the layer underneath, which in the Antarctic is generally composed of coarse-grained and denser snow or firn, or constitutes a layer of ice embedded in-between. In this case comparatively high back-scattered or reflected components must be expected. However, with increasing thickness of the dry snowpack the volume dispersion dominates within this layer, which leads to low radar back-scatter values (FAHNSTOCK et al. 1993, SAURER et al. 1998).

In order to be able to attribute radar back-scatter values to near surface features of an ice body, additional data on its glaciological properties and the ice dynamics is required. Regarding the area of Ekströmsisen, various aircraft and in-situ measurements are available apart from different interpretations on optical Landsat MSS imagery (IfAG 1989; IfAG 1993; IfAG/AWI 1994) (cf. Fig. 1). The latter is particularly suited for a synergistic analysis of ERS-1/2 SAR images (BENNAT et al. 1994).

Glaciological interpretation of back-scatter in ERS-1 SAR data

A section of a typical ERS-1 SAR intensity image of the north-western part of Ekströmsisen (Orbit 24343, frame 5085, acquisition date: 11 March 1996; light grey values correspond to high radar back-scatter values) is shown in Figure 2. The ice shelf as well as the bordering ice caps are characterized by significant local variations in the intensity of the back-scattered and reflected radar signal which represent a great variety of topographic and glaciological features. By means of Figure 2 eight different feature types are classified (A1 to A8). Another three categories C1 to C3 can be identified on the adjacent inland ice

Date of recording ERS-1/2	ERS-1 Orbit	ERS-2 Orbit	Frame	Track	Covered area
18/19 Feb 1996	24028	4355	5085	493	Ekströmsisen (E), Halvfarryggen (N)
19/20 Feb 1996	24038	4365	5697	2	Ekströmsisen (SW), Søråsen (E)
11/12 Mar 1996	24343	4670	5058	307	Ekströmsisen (NW), Auståsen, Atka Iceport
09/10 Apr 1996	24758	5085	5103	221	Ekströmsisen (S), Halvfarryggen (S), Ritscherflya (N)

Table 1: List of the ERS-1/2 SAR scenes used for this investigation on Ekströmsisen and the adjacent ice-sheet regions.

Tabelle 1: Zusammenstellung der für diese Untersuchung verwendeten ERS-1/2-SAR-Szenen des Ekströmsisen und der angrenzenden Inlandeisebereiche.

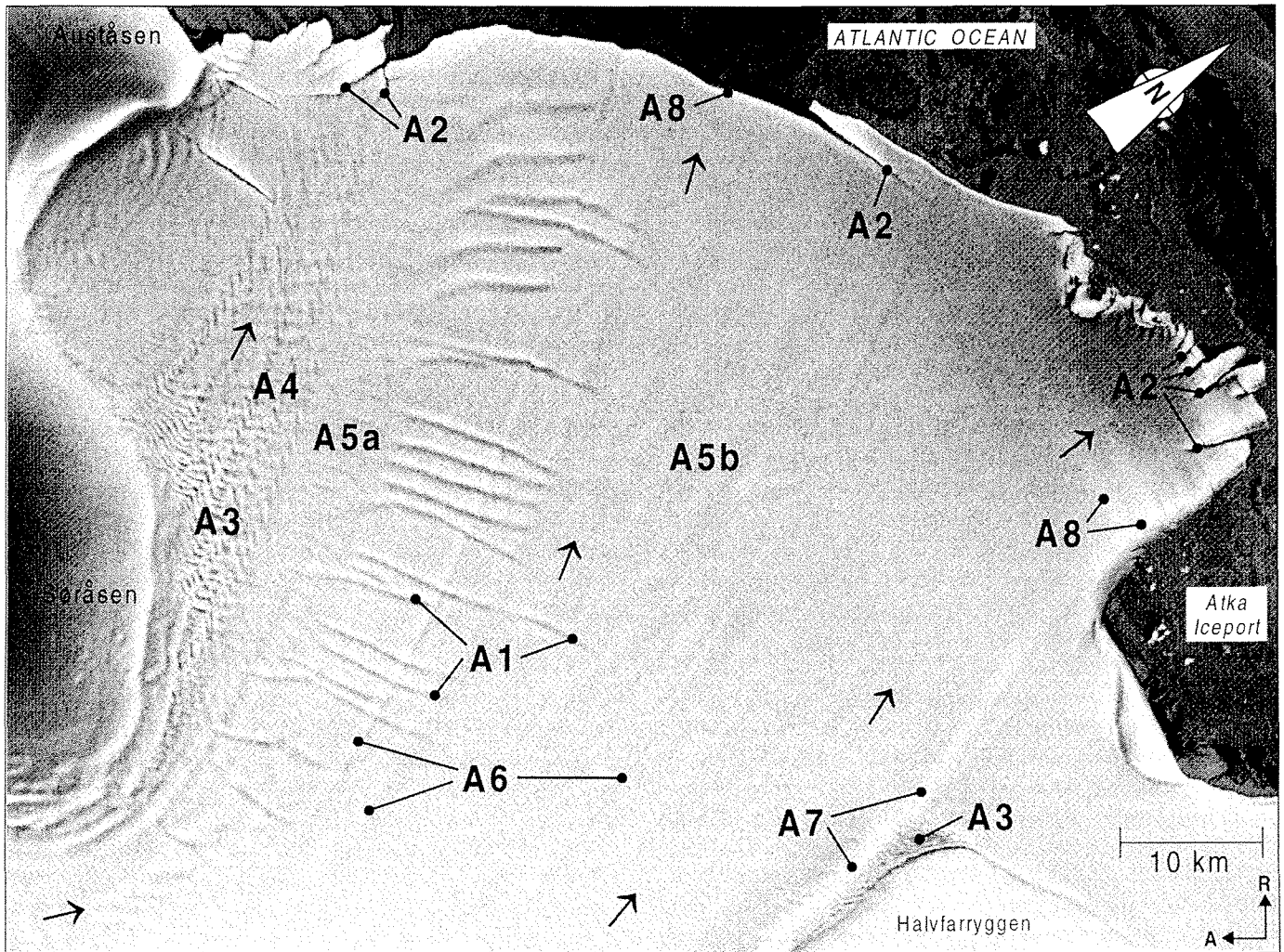


Fig. 2: ERS-1 SAR intensity image of the northwestern part of Ekströmsisen (Orbit 24343, Frame 5085, acquisition date: 11 March 1996). Marked are: rifts (A1), inlets in the ice front (A2), crevassed areas (A3), relics of crevasses and surface undulations filled with snow (A4, A5), flowlines (A6), shear zones (A7), snow cover modified by wind erosion and sea spray (A8). The main flow directions of the ice shelf are indicated by arrows (IfAG 1989, HINZE 1990).

Abb. 2: ERS-1-SAR-Intensitätsbild des nordwestlichen Ekströmsisen (Orbit 24343, Frame 5085, Aufnahme datum: 11.03.1996). Markiert sind: Schelfeisgräben (A1), Eisfrontkerben (A2), Spaltengebiete (A3), Spaltenrelikte und schneeverfüllte Oberflächenundulationen (A4, A5), Fließlinien (A6), Scherzonen (A7), kantennahe Bereiche mit veränderter Deckschicht durch Winderosion und Seewassergischt (A8). Die Hauptfließrichtungen des Schelfeises sind durch Pfeile angezeigt (IfAG 1989, HINZE 1990).

sheet (Fig. 4).

Long-stretched structures (A1) appear over a distance of (~60 km) on western Ekströmsisen. Most of them are aligned parallel and oriented perpendicular to the flow direction of the ice shelf. Comparisons with interpreted Landsat MSS imagery (IfAG 1989) (Fig. 1) identify these features as rifts having a length of up to 18 km and a spacing of 1-6 km. Electromagnetic ice thickness measurements indicate a local thinning of the ice body along the rifts (SANDHÄGER & BLINDOW 2000) which mark potential lines of weakness in the ice shelf (SWITHINBANK et al. 1988). The formation of the rifts of Ekströmsisen occurs directly east of the particular zone of concentrated ice flux from the Søråsen ice cap into the ice shelf (cf. Fig. 1). The ice masses are strongly accelerated there, and the direction of flow is turning by about 90° from west-east to nearly south-north (Fig. 4). Since the resulting lateral extension of the ice body can probably not

be fully compensated by regular ice-shelf thinning, rifts are generated in this area (cf. ROBIN 1958). From here, these structures will be carried off to the ice front.

Inlets (A2) break along the ice-shelf front as a result of abrupt stress reduction in highly stretched seaward parts of the ice body or due to high strain caused by an one-sided lateral coupling to the topography. These inlets appear on radar imagery as well as on optical Landsat MSS recordings as high-contrast linear structures, reaching as far as the water surface (IfAG 1989) (Fig. 1). The frequency and the courses of the inlets allow conclusions on the calving dynamics of different coastal sectors (cf. Fig. 5 and explanatory text).

Primarily to the northeast of Søråsen, but also directly to the northwest of Halvfarryggen, closely spaced structures of comparatively high contrast appear (A3) which are mainly oriented

perpendicular to the flow direction of the ice shelf. From Landsat MSS recordings and terrestrial observations it is known that these structures are surface crevasses (IfAG 1989) (Fig.1). They are resolved even more clearly in ERS SAR intensity images than by optical satellite imagery.

Glaciological features of the category A4 lack contrast and are less sharp as compared with those of category A3; moreover, they run in most cases nearly diagonally to the flow direction of the ice shelf. Between the northeastern margin of Søråsen and the ice front these features form a narrowly structured pattern, presenting in the direction of flow a continuous transition from the structural features of category A3 to those of category A4. From this it can be concluded that the open surface crevasses (A3) are carried off from their area of origin and are either refilled by precipitation or close up due to the flow properties of the ice. These relics of crevasses (A4) are hardly traced on the surface topography and cannot be identified on Landsat MSS imagery (IfAG 1989).

Other areas of Ekstrømsisen are imaged as low-contrast and unsharp undulations, which may present relatively dense structures oriented almost perpendicular to the ice-shelf flux (A5a) or may run parallel with the direction of flow (A5b), as is the case with the longer undulated structures in the central part of western Ekstrømsisen. On Landsat MSS recordings no such surface features can be identified (IfAG 1989). The long-stretched zone A5a forms a transitional area between two differently structured regions. The crevasses and crevasse relics located to the west as well as the rifts adjoining to the east point to complex stress conditions in the ice which might cause deformations varying at a small-scale range. The appearance of the large longitudinal features of category A5b still needs explanation.

Another important glaciological phenomenon are flowlines (A6) which are needed to determine the flow regime of the ice shelf in detail. Flowlines represent in one respect boundary lines between ice masses of different origin. Thus, in Figure 4 two central flowlines stand out in the western part of Ekstrømsisen, each of which can be followed from its point of origin at the grounding line to as far as the ice-shelf front. These flowlines delimit the three main catchment areas of the ice shelf in the south and the west, respectively. On the other hand, flowlines seem to result also from the bedrock topography in the grounding zones. On optical satellite imagery flowlines could unambiguously be identified only in the southern and central parts of Ekstrømsisen (Fig.1). However, in radar intensity images these glaciological features of category A6 can be followed continuously up to the ice front (Fig.2). Since radar systems facilitate additionally the detection of near surface structures, also such sections of flowlines appear in the radar data which have been more and more covered by precipitation and drifting snow with increasing distance from their points of origin. In optical satellite images these sections are no more visible.

The long-stretched zone of high radar reflection (A7, bright strip), which runs nearly parallel with the northwestern grounding line

of Halvfarryggen and extends as far as the Atka Iceport, constitutes a characteristic reproduction of a shear zone (BENNAT et al. 1994, VAUGHAN et al. 1994, GROSFELD et al. 1998, RIGNOT & MACAYEAL 1998). Surrounded by surface crevasses and/or crevasse relics in its southern part, the shear zone has a width of almost 2 km in some places. High horizontal shear stresses within this zone cause fragmentary breaks of at least the upper part of the ice body. This leads to increased radar scattering and reflectivity causing the high signal intensity in the ERS SAR image. Since shear zones, which can be a considerable contributory factor to the flow regime of an ice shelf (GROSFELD et al. 1998, MACAYEAL et al. 1998), are often covered by a layer of snow, it is generally not possible to identify them in optical satellite imagery (BENNAT et al. 1994, VAUGHAN et al. 1994). Hence, the shear zone A7 could not be classified in the relevant Landsat MSS images (IfAG 1989) (comp. Fig. 1 with Fig. 4), but it is discernible in corresponding radio-echo sounding profiles (cf. ROSENBERGER et al. 1995).

Directly by the ice-shelf front a clearly increased radar back-scattering is recorded (A8). On the one hand it indicates changes in the structure of the surface layer, which are due to erosion of snow by wind. This effect is particularly evident to the west of the Atka Iceport, where in the main wind direction (KÖNIG-LANGLO 1992; KÖNIG-LANGLO & HERBER 1996) the wind has clearly modified the snowpack in several zones extending towards the inland over distances of up to 10 km. On the other hand the occurrence of sea spray at the ice front causes an input of humidity into the surface layer and effectuates its crusting, thus producing another increase of radar back-scattering.

ERS-1/2 SAR differential phase image mosaic of Ekstrømsisen

The radar systems of ERS-1 and -2 record the intensities (amplitudes) and the phase relations of the back-scattered and reflected signal. Two data sets acquired at different times and/or with slightly different look angles of the sensors allow under certain circumstances (i.e. coherence of the signal, precision of image matching) to calculate a differential phase image and/or an interferogram (GABRIEL et al. 1989, GOLDSTEIN et al. 1993). The representation of lines of the same phase difference by means of colour or grey value codes shows the typical interferometric patterns (‘fringes’) (Fig. 3).

As it concerns the recorded features, the value of the interferometric phase is particularly influenced by four factors (RIGNOT 1996): surface topography, velocity of the ice, tide-dependent vertical movements, and curvature of the earth surface. With regard to glacio-kinematic studies only the horizontal surface movements of the ice and the tidal amplitude of the floating ice shelf are of special interest.

The flow direction of the ice can best be captured by interferometric phases, if the range direction of the sensor system and the flow direction are coincident as far as possible. Due to the variations in flow direction occurring on Ekstrømsisen and the adjacent regions of grounded ice, the derivation of differential phase images was applied to ERS-1/2 SAR data of descending

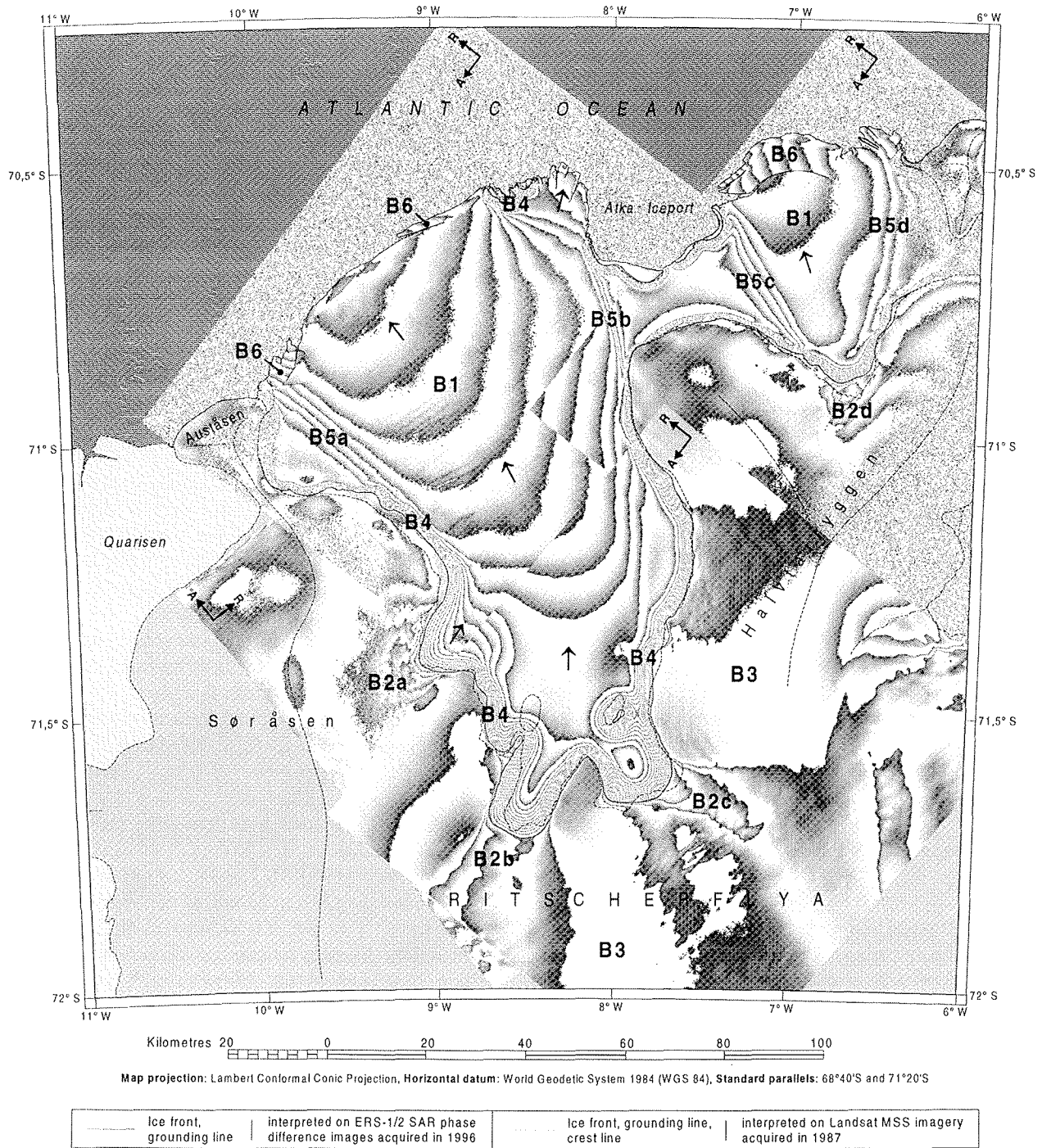


Fig. 3: Mosaic of four ERS-1/2 SAR differential phase images of Ekströmisen and the adjoining ice-sheet regions (24 h time interval; cf. Tab. 1). Phase differences caused by topography and earth curvature are removed. Classification of the interferometric patterns: Central ice-shelf regions (B1); zones of concentrated ice flux from inland into Ekströmisen (B2); grounded ice showing little surface movement (B3); narrow, closely spaced fringes (B4) used to define the grounding line; zones of increased horizontal shear stress, possibly with hinge-like behaviour when under tidal influences (B5); partially detached ice plates at the ice-shelf front (B6). The courses of the grounding lines interpreted from Landsat MSS imagery (IfAG 1989, IfAG 1993, IfAG/AWI 1994) are added for comparison. For each SAR image the flight direction (azimuth: A) of the satellites and the direction of recording (range: R) of the SAR sensors are indicated. Fringes cannot be generated in regions without any coherence between ERS-1 and ERS-2 SAR data (e.g. for the open ocean). Arrows indicate the main flow directions of the ice shelf (IfAG 1989, HINZE 1990).

Abb. 3: Mosaik aus vier ERS-1/2-SAR-Phasendifferenzbildern des Ekströmisen und der angrenzenden Inlandeisebereiche (Beobachtungsintervall: 24 h; vergl. Tab. 1). Die durch die Topographie und Erdkrümmung hervorgerufenen Phasendifferenzen sind eliminiert. Klassifizierung der interferometrischen Muster: zentrale Bereiche des Schelfeises (B1); Hauptabflusszonen der Inlandeismassen (B2); Inlandeis mit geringer Oberflächenbewegung (B3); schmale enggescharte Fringes (B4), anhand derer die Aufsetzlinie festgelegt wurde; Zonen erhöhter horizontaler Scherspannung ggf. mit scharnierartigem Verhalten bei Tideneinfluss (B5); teilweise abgelöste Eistafeln an der Schelfeisfront (B6). Zum Vergleich sind die in Landsat-MSS-Aufnahmen interpretierten Verläufe der Aufsetzlinien (IfAG 1989, IfAG 1993, IfAG/AWI 1994) mit eingetragen. Für jedes SAR-Bild sind die Flugrichtung (Azimut) der Satelliten und die Aufnahmerichtung (Range) der SAR-Sensoren angegeben. Besteht keine Kohärenz zwischen ERS-1 und ERS-2-SAR-Daten, ist für die entsprechenden Gebiete eine Generierung von Fringes nicht möglich (z.B. für Wasserflächen). Pfeile deuten die Hauptfließrichtungen der Schelfeismassen an (IfAG 1989, HINZE 1990).

orbits (NE-SW flights) and of ascending orbits as well (SE-NW flights) (Tab. 1, Fig. 3). The preceding step was to separate the interferometric phase components resulting from the surface topography and the earth curvature. For that purpose a digital elevation model derived from airborne altimetry (SANDHÄGER & BLINDOW 2000) was used. The remaining phase differences show therefore only effects due to the horizontal movement of the ice and the tide-dependent vertical displacement of the ice shelf.

A further separation of these movement components and a calculation of the velocity of the ice flow requires a model which takes into account the time-dependent and locally varying effects of the tide on the elastic ice-shelf plate. The limited knowledge of the inner structure of Ekströmisen and the complex topography bordering the ice shelf at the grounding lines did not allow a sufficiently precise determination of a tide model. For this reason the existing data has been preferably analysed in a qualitative way, but also used for first quantitative estimations.

A mosaic of Ekströmisen and the adjacent ice caps and ice-sheet regions was assembled from four differential phase images of ERS-1/2 (Fig. 3). The necessary rectification of the imagery is based on some few control points and a terrain model of limited accuracy. Close to the ice front of western Ekströmisen the positional deviations of the mosaic amount to about 100 m related to geo-referenced Landsat MSS data, but it is supposed that they will increase in eastern and southern directions where additional ground control is lacking.

Flat ice-shelf regions with high and nearly horizontal flow velocities are rendered in the interferograms by concavely shaped fringes arranged in a comparatively dense and regular order (B1). These fringes represent the typical pattern for the velocity field of the ice-shelf flow. The highest surface velocities exist along the middle axes of these patterns where the distances between successive fringes in range direction are small. The velocities decrease continuously towards the edges of the ice shelf, i.e. the distance between two fringes increases referring to the range direction. Moreover, it can clearly be seen that the velocity of the eastern part of Ekströmisen is only about the half of that of the western main part.

The four particular zones of high ice flux from inland into Ekströmisen are characterized by interferometric patterns of irregular, but mostly concave fringes (B2a - B2d). In these regions the velocity of the inland ice masses significantly increases when approaching the grounding line (MAYER 1996), which can clearly be seen in the fringe patterns B2a, B2c, and B2d. Here the main axes of these zones of concentrated ice flux are oriented nearly parallel to the range direction of each single SAR image, i.e. the fringes render a great part of the ice motion. In contrast to this, the main flow direction of the ice in the southwesternmost zone (B2b) is not coincident with the range direction but with the azimuth direction of the corresponding intensity image. That is the reason why the concave fringe pattern exists only in an rudimentary way inland of the grounding line. Summarised it can be seen that using adequate interferograms a relatively

simple identification of marked zones of high ice flux from the ice-sheet regions into the ice shelves is possible.

Vast regions of the ice domes and of Ritscherflya on the southern border of Ekströmisen show broad spaced fringes (B3). These fringe patterns indicate relatively small surface velocities of the ice movement of some few meters per year. The often irregular shapes of the fringes are supposed to be due to residual topographic influences, but they can nevertheless result from small-scale flow effects, like e.g. in regions with a distinct subglacial bedrock relief (SANDHÄGER & BLINDOW 2000).

Contrary to the grounded inland ice sheet a floating ice shelf is subjected to tidal vertical movements which can cause significant periodical changes of the surface slope around the grounding line. This explains why the interferograms show the narrow spaced fringe zones (B4) going along the grounding line. The number of fringes is proportional to the amount of the tidal amplitude within the observation interval. According to GOLDSTEIN et al. (1993) those fringe patterns are well-suited to set precisely the position of the grounding line with an accuracy of up to (± 0.5 km). With this, uncertainties which remain in the mapping of optical satellite recordings or of ERS-1/2 SAR intensity images can substantially be reduced.

Figure 3 gives the courses of the grounding lines interpreted not only by means of the ERS-1/2 SAR differential phase image mosaic, but also with Landsat MSS recordings acquired in 1987 (IfAG 1993, IfAG/AWI 1994). Good coincidence can be found especially for those parts of the grounding line which are only passed by small ice mass fluxes. Here a considerable change of the surface slope takes place along the transition from ice shelf to grounded ice (SANDHÄGER & BLINDOW 2000), which is visible in optical satellite image data as a striking line. At the northeastern margin of Søråsen and along the four particular grounding-zone sections characterized by comparatively high ice fluxes (cf. Fig. 1) the interpreted grounding lines show significant lateral deviations of up to (~ 5 km). The discrepancies result above all from misinterpretation on the Landsat MSS imagery, because the grounding zones there show slope changes of the surface which are either smaller or do not directly correlate with the inland ice/ice-shelf transition. The same is true for the southwestern part of Ekströmisen, where two ice rumpled (with a total area of (~ 35 km²) had incorrectly been identified in the Landsat MSS imagery, whereas the fringe pattern in the ERS-1/2 SAR interferogram indicates only one small ice rumple of ~ 3 km².

Figure 3 shows along the lateral margins of the central northwestern and eastern parts of Ekströmisen striking interferometric patterns (B5a-d) consisting of relatively narrow-cut fringes going approximately parallel to the main flow direction. So, on the one hand, the existence of increased horizontal shear stress must be attended along these fringe patterns. The reason for this shear stress is an interaction between the relatively rapidly moving ice-shelf masses of central western and eastern Ekströmisen and the significantly slower moving ice-shelf portions which are laterally coupled to the ice domes or the different ice rises

and ice rumples (HINZE 1990, DETERMANN 1991). Therefore the shear zone A7 identified in the ERS-1 SAR intensity image (Fig. 2) is directly coincident with the fringe pattern B5b. On the other hand each of the interferometric patterns B5a-d connects two points of the lateral margins of Ekströmisen where the ice-shelf plate is supposed to be mounted in a hinge-like manner, so tide effects along these 'hinges' would cause similar periodic changes of the surface tilt like along the grounding line. But in a differential interferogram calculated by MÜLLER et al. (1997) for northwestern Ekströmisen, which represents only those components of phase differences resulting from the tide-dependent vertical movements of the ice shelf, none of the two fringe patterns B5a and B5b are discernible. As a consequence the above mentioned flow-dynamic effects could only be the principal reason for the nature of these two patterns (and not the tidal effect).

The ice-shelf region situated between the northwestern part of Halvfarryggen and the Atka Iceport is completely laterally limited by the fringe patterns B5b and B5c. It is supposed that nearly no coupling to western and eastern Ekströmisen does exist regarding the geometry of the ice body (SANDHÄGER & BLINDOW 2000) and the ice dynamics. Consequently these two parts of Ekströmisen represent two independent ice-shelf systems.

Ice-shelf fragments at the ice front (B6) which are for large parts separated from the ice shelf and are coupled to it only at one side, are reacting otherwise to tidal influences than the ice shelf itself. So different interferometric patterns arise (Fig. 3) the fringes of which stand out from the fringe pattern of the adjacent ice-shelf areas by a narrower spacing and another direction. Taking the arrangement of the inlets in the ice front into account, it is possible to give by means of interferograms some statements on the extent of the calving area expected to break off. Possible future tabular icebergs are identifiable at three points at the ice front of western and eastern Ekströmisen with the help of the fringe patterns B6. The eastern and greatest one covers an area of (~160 km², that corresponds to approx. 8 % of the total area of eastern Ekströmisen (IfAG 1989).

ERS-1 SAR intensity image mosaic of Ekströmisen

Figure 4 shows an intensity image mosaic made of ERS-1 SAR data acquired of Ekströmisen and the adjoining inland ice regions in 1996 (Tab. 1). The mosaic shows the following topographic characteristics and glaciological forms which have been classified and mapped in SAR intensity images and differential phase images: grounding lines, ice fronts, flowlines, shear zones, rifts, crevasses and crevasse relics, surface undulations on the ice shelf, ice rumples, and crest lines. Compared to the glaciological map of Ekströmisen, published in 1989 by IfAG (1989; cf. Fig. 1), which was derived from Landsat MSS images, it is evident that Figure 4 represents significantly more detailed and a greater number of glaciological forms and is more precise as to feature position. In Figure 4 three more characteristic features (C1 to C3) can be distinguished and be correlated to glaciological forms of the inland ice regions.

The central regions of Søråsen and Halvfarryggen are characterised by a very low back-scatter intensity of the radar signals, which appears on the intensity image mosaic as dark grey to black areas (C1). On these ice domes the average annual snowfall can definitely amount to more than 0.5 m_{snow} a⁻¹ (SCHLOSSER et al. 1999). Because of their higher elevations (600 m to 700 m), the average annual surface temperatures of the ice domes are beneath those of the ice-shelf region. Since even the Antarctic summer causes no surface melting, it is supposed that a thick and nearly homogeneous snow cover exists which is only interrupted by singular layers of deep hoarfrost (pers. comm. M. Lange & S. Eickschen, 1997). Here the radar signal can penetrate deep into the snowpack, what explains the low back-scattered signal to the SAR sensor.

Although surface elevations and snow-accumulation rates in the area of the Ritscherflya ice-sheet slope bordering on Ekströmisen in the south amount approximately to those of the central ice-dome regions (Fig. 1; OERTER et al. 1997), Figure 4 shows a significantly higher back-scatter intensity of the radar signals there. One reason might be the occurrence of an accelerated densification of the snowpack due to increased near surface strain rates and longitudinal stresses (cf. ALLEY & BENTLEY 1988) which are caused by the clearly converging inland ice movement in this catchment area. The converging character of the flow regime is depicted particularly in the concentrated ice discharge from Ritscherflya into southern Ekströmisen through two relatively narrow zones (Fig. 1). Moreover the increased surface roughness, connected with discernible surface undulations (feature type C2, see below), as well as a hardening of the surface layer resulting from aeolian influences, as e.g. katabatic winds, possibly contribute to the comparatively high intensity of the radar signals back-scattered and reflected from the northern slope of Ritscherflya.

On the ERS-1 SAR intensity images the flat ice-shelf regions and the marginal zones of the adjacent ice domes also appear as medium to light grey areas of high signal intensity. Here, slight surface melting during the Antarctic Summer and subsequent refreezing lead to the formation of thin ice layers and ice lenses. The typical layering of the snowpack and the firn therefore results from an alternation of fine-grained winter snow and coarse-grained summer snow, partly interspersed with such ice layers and lenses (e.g. ROSENBERGER et al. 1997, SCHLOSSER et al. 1999, pers. com. M. Lange & S. Eickschen 1997, and H. Oerter 2000). These inclusions constitute effective reflectors and diffractors for radar radiation.

Several marginal zones of the ice domes and nearly the whole region of Ritscherflya are characterised by small-scale intensity variations (C2). These structures are correlating with surface undulations which could also be detected on Landsat MSS imagery (IfAG 1989) as well as in geodetic elevation-profile measurements (KARSTEN & RITTER 1990, MAYER 1996). The undulations are being structured partially regularly, partially densely, but predominantly perpendicular to the flow direction (Fig. 1). The average wave length is between 3 km and 5.5 km, which is about three to nine times the amount of the local ice

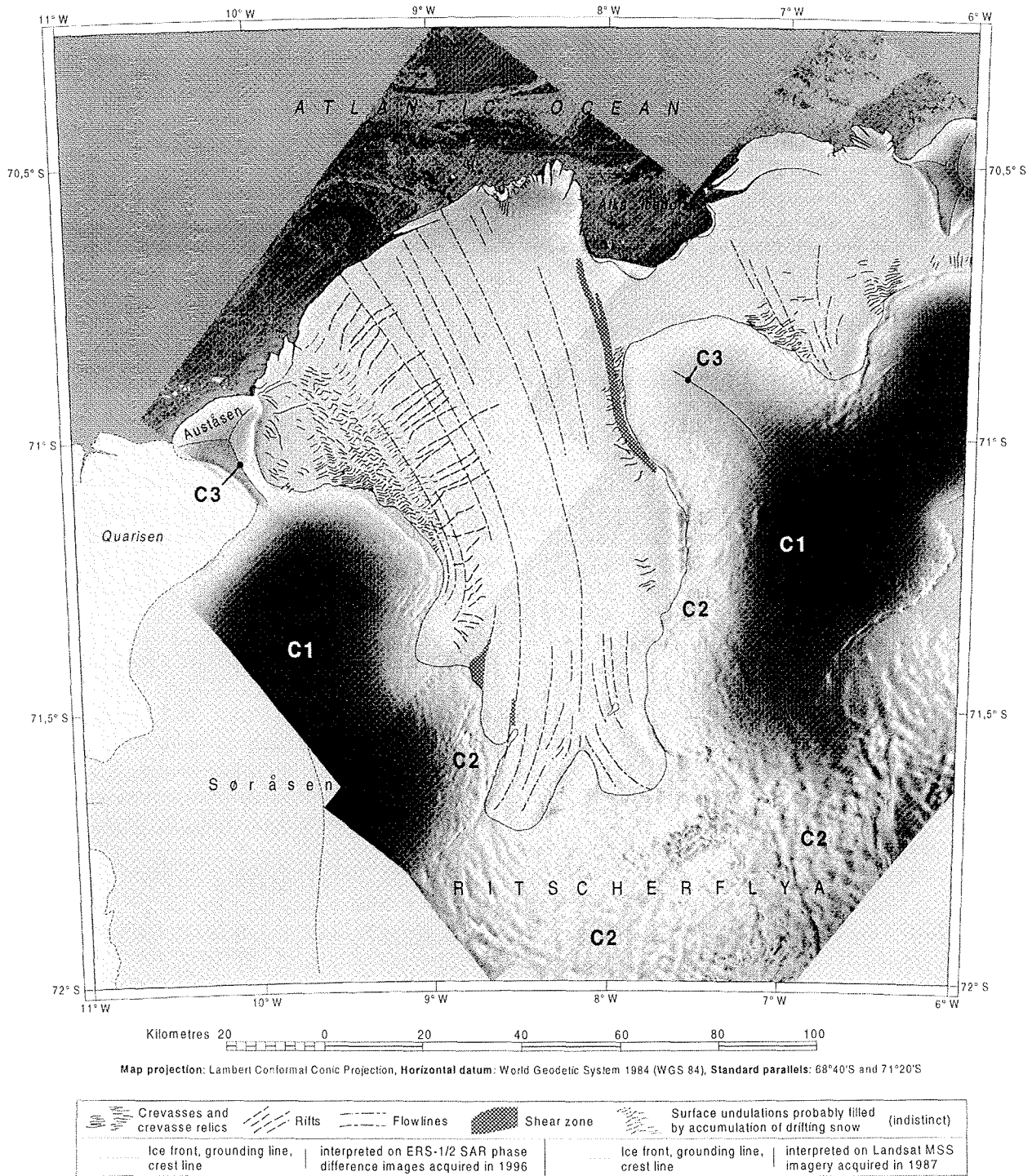


Fig. 4: Mosaic of four ERS-1 SAR intensity images and topographic-glaciological map of Ekströmsisen and the adjoining ice-sheet regions (cf. legend of the map). C1: Areas of grounded ice showing very low radar back-scattering; C2: Surface undulations causing high radar back-scattering; C3: Crest lines or ice divides. Represented results of interpretations on Landsat MSS imagery are adopted from IfAG (1989, 1993) and IfAG/AWI (1994).

Abb. 4: Mosaik aus vier ERS-1-SAR-Intensitätsbildern und topographisch-glaziologische Karte des Ekströmsisen und der angrenzenden Inlandeisbereiche (vergl. Kartenlegende). C1: Inlandeisregionen mit sehr geringer Radarrückstreuung; C2: Oberflächenundulationen, die eine hohe Radarrückstreuung bewirken; C3: Kamm-linien bzw. Eisscheiden. Quellen der in Landsat-MSS-Aufnahmen interpretierten und hier eingetragenen Oberflächenmerkmale: IfAG (1989, 1993), IfAG/AWI (1994).

thickness, respectively (SANDHÄGER & BLINDOW 2000). According to GRAF et al. (1990) and OERTER et al. (1997), variations of the accumulation rate of drifting snow are resulting from an ice-surface relief structured of that kind, at least in the region of Ritscherflya bordering the southern part of Ekströmsisen. That would explain why this type of topographic feature in general appears clearer in ERS-1/2 SAR intensity images than in optical satellite imagery. In-situ elevation measurements carried out by KARSTEN & RITTER (1990) and MAYER (1996) indicate an average height difference of the surface undulations of ~15 m.

While SEKO et al. (1993) attributes the formation of such surface undulations to effects which are primarily caused by the subglacial bedrock relief, WHILLANS & JOHNSEN (1983) underline the significant influence of very small variations in the basal sliding velocity of the ice sheet on its small-scale surface relief. In the catchment area of Ekströmsisen the ice-sheet base shows mainly small elevation changes in those regions where ice-surface undulations appear (SANDHÄGER & BLINDOW 2000). According to MAYER (1996), however, a tendency towards basal sliding exists with diminishing distance from the grounding line, at least in the area of the southwesternmost grounding zone of Ekströmsisen. Therefore it must be supposed that the surface undulations C2 result from a combined influence on the ice dynamics not only by the subglacial bedrock relief, but also by sliding processes at the ice/bedrock transition. The effects of aeolian influences, as e.g. katabatic winds, on the formation of these surface features is not yet clearly defined.

Nevertheless, a surface characteristic is supposed to be found for inland ice regions which is relatively simple to identify and map on satellite imagery. At the same time it allows to make first conclusions on the ice-dynamic conditions prevailing at the ice/bedrock transition. This is important, as basal sliding is in

particular controlling the movement of the grounded ice masses and their flow regime. Up to now this influencing parameter could directly be measured only with great effort and only at singular spots.

Another feature which appears only with an adequate direction of radar illumination in SAR data are crest lines (C3). These topographic features, however, are often clearer to recognise in optical satellite images (IfAG 1989, VAUGHAN et al. 1994). A precise knowledge of the traces of crest lines is important especially for studies of the dynamics of the inland ice and its flow regime, as such structures are marking the position of ice divides, thus the lateral edges of drainage systems (e.g. DREWRY 1983).

Dynamics of the ice-shelf front

An essential part of the accumulation of ice on the Antarctic continent is balanced by calving of icebergs along the ice-shelf edges (JACOBS et al. 1992). The mean annual mass loss due to calving events is therefore an important mass balance quantity of the relevant drainage system. This quantity can be roughly estimated from the time-dependent ice-front fluctuations and the ice-thickness distribution there.

Figure 5 shows the positions of the ice front of Ekströmsisen in October 1987 and in February/March 1996 as mapped from Landsat MSS recordings (IfAG 1993, IfAG/AWI 1994) and ERS-1/2 SAR images (Tab. 1), respectively. Those regions which were free of ice in 1987 and occupied by the ice shelf in 1996 are marked in white; regions which were covered with ice in 1987 and free of ice in 1996 are marked in black.

The central coastal sectors A of the western and the eastern part

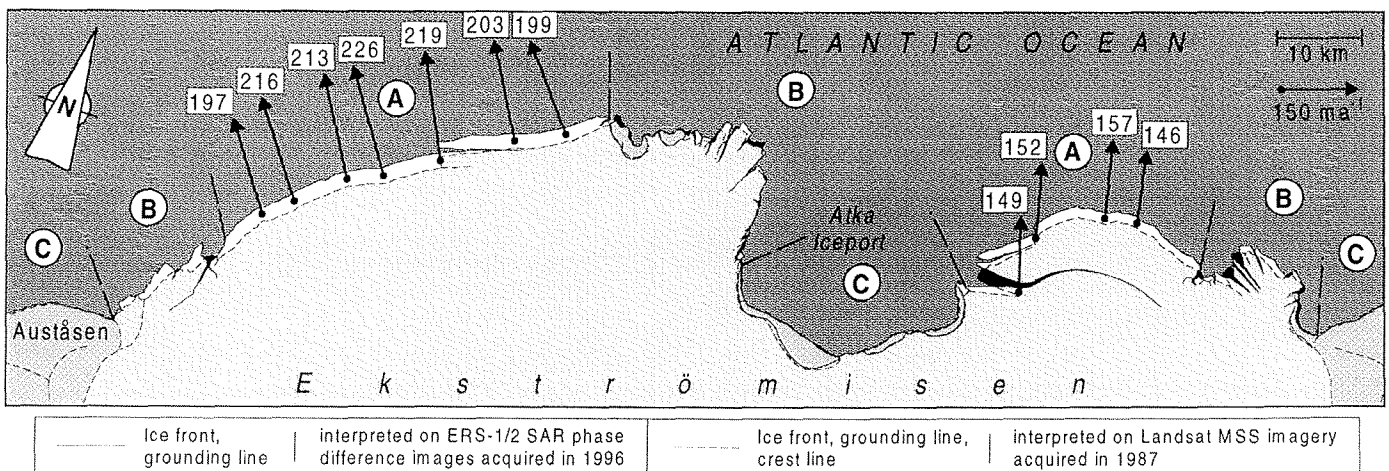


Fig. 5: Changes of the ice front of Ekströmsisen between 1987 and 1996 (white: areas free of ice in 1987 and covered by ice in 1996; black: areas covered by ice in 1987 and free of ice in 1996). The subdivision of the coastal zone into sectors A, B, and C is explained in the text. The mean annual advance between 1987 and 1996 is given for selected locations along the ice-front sections A. Represented results of interpretations on Landsat MSS imagery are adopted from IfAG (1989, 1993) and IfAG/AWI (1994).

Abb. 5: Lageänderung der Eisfront des Ekströmsisen zwischen 1987 und 1996 (weiß: 1987 noch eisfreie, 1996 dann vom Eiskörper überdeckte Bereiche; schwarz: 1987 eisüberdeckt, 1996 wieder eisfrei). Die Unterteilung der Küstenzone in Abschnitte A, B und C ist im Text erläutert. Für ausgewählte Punkte entlang der Eisfrontabschnitte A ist der mittlere jährliche Kantenvorschub zwischen 1987 und 1996 angegeben. Quellen der in Landsat-MSS-Aufnahmen interpretierten und hier eingetragenen Oberflächenmerkmale: IfAG (1989, 1993), IfAG/AWI (1994).

of Ekströmisen are characterised by an ice front that has advanced in a relatively regular way between 1987 and 1996. The shape of the front has not significantly changed between these years. This indicates that only a small loss of ice masses due to calving occurred during the period of observation. In the western central part, the average annual advance of the ice front has been approx. 200-230 m, and up to ~150 m in eastern Ekströmisen. The values determined for the western part agree well with directly measured velocities of the ice-shelf flow (IfAG 1989, HINZE 1990) within $\pm 5\%$. Such a comparison with in-situ measurements is not yet available for the eastern part.

The alignment of rift structures parallel to the ice front indicates that along the coastal sections A predominantly calving of large tabular icebergs occurs after long periods of presumably several decades without considerable calving activity. A large calving event took place in 1980 in the central western part (IfAG 1989). Another large calving event will occur most likely in the near future in the eastern part of Ekströmisen (comp. Fig. 1 and Fig. 5).

The coastal sectors marked B in Figure 5 show between 1987 and 1996 irregular changes of the position of the ice front with partial advancing, withdrawal or also apparent stagnation. The relatively rough ice-shelf edges indicate a low age of the ice front. Number and extent of the numerous inlets have definitely increased. As a consequence it seems that at these coastal parts B regular calving of small icebergs occurs in a shorter time interval. Estimation of the near-edge velocities of the ice-shelf flow from satellite imagery is thus impossible in such regions.

The coastal sectors C are characterized by small differences between the ice-front positions recorded in 1987 and 1996. The ice fronts in these sectors are ice cliffs bounding grounded and nearly stagnant ice masses (HINZE 1990). This leads to an only small mass flux which is compensated by the break-off of small icebergs and by melting processes at the ice front.

Based on the derived advance rates of the ice front it is possible to estimate in a first approximation the mean annual mass loss due to calving or near-edge melting. Together with the ice-thickness distribution in the coastal region (SANDHÄGER & BLINDOW 2000), we postulate for the western part of Ekströmisen a seaward ice flux of $\sim 2.7 \text{ km}^3 \text{ a}^{-1}$. An estimation by KIPFSTUHL (1991) gives a value of $\sim 2.4 \text{ km}^3 \text{ a}^{-1}$. In the smaller eastern part of Ekströmisen, the seaward ice flux amounts to only $0.9 \text{ km}^3 \text{ a}^{-1}$. Hence, if the tabular iceberg, largely decoupled already in 1996, would completely break off, this part of the ice shelf would lose a mass of ice by a single calving event which is about a 35 times as much as the estimated annual average.

CONCLUSIONS

SAR intensity images and differential phase images are efficient tools of remote sensing to investigate glaciological surface characteristics and dynamic effects for an ice shelf. The method of glacio-kinematic interpretation of such image data is an ideal

supplement for the already well established procedures of evaluation of optical satellite image data. For the time being, relatively great effort is necessary to record, process and analyse the SAR data. In the near future we hope to considerably reduce these problems. Thus it will be possible to have all the advantages of the SAR technique operating independent from daytime and weather with reduced effort of the user.

A substantial progress is above all to integrate interferograms into the interpretation for a detailed definition of the courses of grounding lines. This is important as in the transition zone between inland ice sheet and ice shelf the characters of the velocity field of the ice flow and of the stress field within the ice are significantly changing (transition from ice movement controlled by shear stress to an ice flow controlled by tensile stress). This has to be considered, e.g. when using numerical flow models to simulate the ice dynamics, or when defining the mass flux over the grounding line - a fundamental quantity in the budget of Antarctic drainage systems. On the other hand, it is the position of active grounding zones with relatively high ice fluxes which is judged as being sensitive for a climatic change. Analyses of interferometric data from long-term repetitive acquisitions should allow to detect also very small changes of the mass flux and/or of the ice thickness within the grounding zones.

Moreover, the procedure of a combined interpretation of SAR intensity images and interferograms could be applied for large-scale monitoring of Antarctic key regions in order to reveal changes in principal glaciological characteristics, such as the ice-shelf flow regime (depicted particularly in the interferometric fringe patterns, the trajectories of flowlines, the distribution of fractures and rifts) and the ice-front calving rate (indicated by an irregular advance/retreat of the ice front and/or by alterations in the dynamics of the ice-shelf frontal zone).

ACKNOWLEDGEMENTS

The glacio-kinematic interpretation of the ERS-1/2 SAR data was carried out within the framework of the Project No. 03PL016A entitled "Investigating dynamic snow and ice processes of various Antarctic geosystems by means of remote sensing techniques (DYPAG)", a joint project sponsored by the Bundesministerium für Bildung, Wissenschaft, Forschung und Technologie (bmb+f) der Bundesrepublik Deutschland. The necessary ERS data were made available free of charge in the course of the research project AO2.D149 "Monitoring dynamic processes in Antarctic geosystems (MODPAG)", sponsored by ESA. We wish to thank H. Oerter and an anonymous reviewer for helpful comments on the manuscript.

References

- Alley, R.B. & Bentley, C.R. (1988): Ice-core analysis on the Siple Coast of West Antarctica.- *Ann. Glaciol.* 11: 1-7.
- Bennett, H., Heidrich, B. & Sievers, J. (1994): Extraction of Antarctic topographic-glaciological features from ERS-1 SAR data.- *Proc. Second ERS-1 Sympos.* - Space at the Service of our Environment, Hamburg, 11-14 October 1993, ESA SP-361: 141-145.

- Determann, J.* (1991): Das Fließen von Schelfeisen – numerische Simulationen mit der Methode der finiten Differenzen.- Ber. Polarforsch. 83: 83 pp.
- Doake, C.S.M. & Vaughan, D.G.* (1991): Rapid disintegration of the Wordie Ice Shelf in response to atmospheric warming.- *Nature* 350: 328-330.
- Drewry, D.J.* (1983): Antarctica: glaciological and geophysical folio.- Scott Polar Research Institute, Cambridge.
- Emery, W.J. & Meincke, J.* (1986): Global water masses: summary and review.- *Oceanologica Acta* 9(4): 383-391.
- Fahnestock, M., Bindshadler, R., Kwok, R. & Jezek, K.* (1993): Greenland Ice Sheet surface properties and ice dynamics from ERS-1 SAR imagery.- *Science* 262: 1530-1534.
- Gabriel, A.K., Goldstein, R.M. & Zebker, H.A.* (1989): Mapping small elevation changes over large areas: differential radar interferometry.- *J. Geophys. Res.* 94(B7): 9183-9191.
- Goldstein, R.M., Engelhardt, H., Kamb, B. & Frolich R.M.* (1993): Satellite radar interferometry for monitoring ice sheet motion: application to an Antarctic ice stream.- *Science* 262: 1525-1530.
- Graf, W., Moser, K. & Rott, H.* (1990): Schneeprofile und Flachbohrungen der Ekström- Traverse 1987.- In: H. MILLER & H. OERTER (eds.), Die Expedition ANTARKTIS-V mit FS „Polarstern“ 1986/87, Ber. Polarforsch. 57: 68-76
- Grosfeld, K., Hellmer, H.H., Jonas, M., Sandhäger, H., Schulte, M., & Vaughan, D.G.* (1998): Marine ice beneath Filchner Ice Shelf: evidence from a multi-disciplinary approach.- In: S.S. JACOBS & R.F. WEISS (eds.), Ocean, Ice and Atmosphere - Interactions at the Antarctic Continental Margin, 319-339, Antarctic Res. Series, Vol. 75, AGU, Washington, D.C.
- Hinze, H.* (1990): Zum Einsatz von Satelliten-Positionierungsverfahren für glaziologische Aufgaben in der Antarktis.- Diss. Nr.163, (in German), Institut für Erdmessung der Universität Hannover, 160 pp.
- IfAG* (1989): Maps of ice shelf kinematics, Topographic map and satellite image map 1:500000, Ekströmisen, SR 29-30/SW, Antarctica.- Institut für Angewandte Geodäsie, Frankfurt am Main.
- IfAG* (1993): Topographic map (satellite image map) 1:1000000, Ekströmisen, SR 29-30, Antarctica.- Institut für Angewandte Geodäsie, Frankfurt am Main.
- IfAG/AWI* (1994): Digital topographic Antarctic data base.- Vers. 1.94(G), Institut für Angewandte Geodäsie, Frankfurt am Main, and Alfred-Wegener-Institute for Polar and Marine Research, Bremerhaven.
- Jacobs, S.S., Helmer, H.H., Doake, C.S.M., Jenkins, A. & Frolich, R.M.* (1992): Melting of ice shelves and the mass balance of Antarctica.- *J. Glaciol.* 38(130): 375-387.
- Karsten, A. & Ritter, B.* (1990): Trigonometrisches Nivellement 1987 auf dem Ekström-Schelfeis.- In: H. MILLER & H. OERTER (eds.), Die Expedition ANTARKTIS-V mit FS „Polarstern“ 1986/87, Ber. Polarforsch. 57: 76-81
- Kipfstuhl, J.* (1991): On the formation of underwater ice and the growth and energy budget of the sea ice in Atka Bay, Antarctica.- Ber. Polarforsch. 85, 89 pp.
- König-Langlo, G.* (1992): The meteorological data of the Georg-von-Neumayer-Station (Antarctica) for 1988, 1989, 1990 and 1991.- Ber. Polarforsch. 116, 70 pp.
- König-Langlo, G. & Herber, A.* (1996): The meteorological data of the Neumayer Station (Antarctica) for 1992, 1993 and 1994.- Ber. Polarforsch. 187, 101 pp.
- MacAyeal, D.R.* (1987): Ice-shelf backpressure: from drag versus dynamic drag.- In C.J. VAN DER VEEN & H. OERLEMANS (eds.), Dynamics of the West Antarctic Ice Sheet, 141-160, D. Reidel, Dordrecht.
- MacAyeal, D.R., Rignot, E. & Hulbe, C.L.* (1998): Ice-shelf dynamics near the front of the Filchner-Ronne Ice Shelf, Antarctica, revealed by SAR interferometry: model/interferogram comparison.- *J. Glaciol.* 44(147): 419-428.
- Mayer, C.* (1996): Numerical modelling of the transition zone between an ice sheet and an ice shelf.- Ber. Polarforsch. 214, 151 pp.
- Müller, U., Sievers, J. & Walter, H.* (1997): SAR data exploitation for monitoring Antarctic ice sheets and glaciers - In: H. OERTER (ed.), Filchner Ronne Ice Shelf Programme, Rep.11: 48-50, Alfred-Wegener-Institute for Polar and Marine Research, Bremerhaven.
- Oerter, H., Graf, W. & Schlosser, E.* (1997): Stable isotope contents of near surface firn from Neumayer base towards Dronning Maud Land, Antarctica - In: H. OERTER (ed.), Filchner Ronne Ice Shelf Programme, Rep. 11: 56-64, Alfred-Wegener-Institute for Polar and Marine Research, Bremerhaven.
- Paterson, W.S.B.* (1994): The physics of glaciers.- 3rd ed., Pergamon/Elsevier Science Ltd, Oxford, New York, Toronto, 480 pp.
- Rignot, E.* (1996): Tidal motion, ice velocity and melt rate of Petermann Gletscher, Greenland, measured from radar interferometry.- *J. Glaciol.* 42(142): 476-485.
- Rignot, E. & MacAyeal, D.R.* (1998): Ice-shelf dynamics near the front of the Filchner-Ronne Ice Shelf, Antarctica, revealed by SAR interferometry.- *J. Glaciol.* 44(147): 405-418.
- Robin, G. de Q.* (1958): Glaciology III. Seismic shooting and related investigations. Norwegian-British-Swedish Antarctic Expedition 1949-52.- Scientific Results, 5.
- Rosenberger, A., Oerter, H. & Miller, H.* (1997): Short range radar observations on Ekströmisen, Antarctica - *Polarforschung* 65(1): 1-14.
- Rott, H., Skvarca, P. & Nagler, T.* (1996): Rapid collapse of northern Larsen Ice Shelf, Antarctica.- *Science* 271: 788-792.
- Sandhäger, H. & Blindow, N.* (2000): Surface elevation, ice thickness, and subglacial-bedrock topography of Ekström Ice Shelf (Antarctica) and its catchment area.- *Ann. Glaciol.* 30, (in press).
- Saure, H., Wunderle, S. & Goffmann, H.* (1998): Radarfernerkundung der Antarktischen Halbinsel.- *Geograph. Rundschau* 50, H.2: 71-77.
- Schlosser, E., Oerter, H. & Graf, W.* (1999): Snow accumulation on Ekströmisen, Antarctica, 1980-1996.- Ber. Polarforsch. 313, 137 pp.
- Seko, K., Furukawa, T., Nishio, F. & Watanabe, O.* (1993): Undulating topography on the Antarctic ice sheet revealed by NOAA AVHRR images.- *Ann. Glaciol.* 17: 55-62.
- Swithinbank, C., Brunk, K. & Sievers, J.* (1988): A glaciological map of Filchner-Ronne Ice Shelf, Antarctica.- *Ann. Glaciol.* 11: 150-155.
- Vaughan, D.G. & Doake, C.S.M.* (1996): Recent atmospheric warming and retreat of ice shelves on the Antarctic Peninsula.- *Nature* 379: 328-331.
- Vaughan, D.G., Frolich, R.M. & Doake, C.S.M.* (1994): ERS-1 SAR: stress indicator for Antarctic ice streams.- Proc. Second ERS-1 Sympos. - Space at the Service of our Environment, Hamburg, Germany, 11-14 October 1993, ESA SP-361: 183-186.
- Whillans, I.M. & Johnsen, S.J.* (1983): Longitudinal variations in glacial flow: theory and test using data from the Byrd Station Strain Network, Antarctica.- *J. Glaciol.* 29(101): 78-97.